

Supporting Information

[Bmim]₂SbCl₅: a main group metal-containing ionic liquid exhibiting tunable photoluminescence and white-light emission

Ze-Ping Wang,^{a,b} Jin-Yun Wang,^a Jian-Rong Li,^a Mei-Ling Feng,^a Guo-Dong Zou,^a
and Xiao-Ying Huang^{*,a}

^a State Key Laboratory of Structural Chemistry, Fujian Institute of Research on the Structure of Matter,
Chinese Academy of Sciences, Fuzhou, Fujian 350002, P. R. China.

^b Fuzhou University, Fuzhou, Fujian 350002, P. R. China.

* Corresponding author, E-mail: xyhuang@fjirsm.ac.cn. Fax: (+86) 591-83793727

List of Contents

1. Experimental section

Table S1. Crystallographic data for [Bmim]₂SbCl₅.

2. More structural details

Table S2. Selected hydrogen bonds data for [Bmim]₂SbCl₅.

Figure S1. Hydrogen bonds for each imidazolium cation in **1**.

Figure S2. Hydrogen bonds for each [SbCl₅]²⁻ anion in **1**.

Table S3. Selected Anion- π Interactions data for [Bmim]₂SbCl₅.

Figure S3. The anion- π interactions in the molecule.

Table S4. Structure diagram of [SbX₅]²⁻.

Table S5. Selected bond lengths for [Bmim]₂SbCl₅ (**1**).

3. Theoretical calculations

Table S6. Plots of the frontier molecular orbitals involved in the emission transitions of [Bmim]⁺ and [SbCl₅]²⁻ calculated by TD-DFT method at the B3LYP level.

Table S7. The optimized geometrical coordinates (unit: angstroms) of [SbCl₅]²⁻ in the ground state by DFT method at the B3LYP level.

Table S8. The optimized geometrical coordinates (unit: angstroms) of [SbCl₅]²⁻ in the lowest singlet excited state by DFT method at the B3LYP level.

Table S9. The optimized geometrical coordinates (unit: angstroms) of [Bmim]⁺ in the ground state by DFT method at the B3LYP level.

Table S10. The optimized geometrical coordinates (unit: angstroms) of **[Bmim]⁺** in the lowest singlet excited state by DFT method at the B3LYP level.

Table S11. Partial molecular orbital compositions (%) in the lowest singlet excited state for **[Bmim]⁺** by TD-DFT method at the B3LYP level.

Table S12. Partial molecular orbital compositions (%) in the lowest singlet excited state for **[SbCl₅]²⁻** by TD-DFT method at the B3LYP level.

Table S13. The emission transitions for **[Bmim]⁺** and **[SbCl₅]²⁻**, respectively, by TD-DFT method at the B3LYP level.

Figure S4. The calculated (blue vertical bars) and simulated (black line, implemented by GaussSum) emission spectra of **[Bmim]⁺** at ambient temperature calculated by TD-DFT method at the B3LYP level.

Figure S5. The calculated (blue vertical bars) and simulated (black line, implemented by GaussSum) emission spectra of **[SbCl₅]²⁻** at ambient temperature calculated by TD-DFT method at the B3LYP level.

4. Physical measurements

Figure S6. PXRD patterns of **[Bmim]₂SbCl₅**.

Figure S7. Photoluminescence lifetime curve of **[Bmim]₂SbCl₅**.

Figure S8. TGA curve of **[Bmim]₂SbCl₅**.

Figure S9. DSC curve of **[Bmim]₂SbCl₅**.

Figure S10. Temperature-dependent PXRD of **[Bmim]₂SbCl₅**.

Figure S11. Temperature-dependent PL spectra of **[Bmim]₂SbCl₅**.

Figure S12. Temperature-dependent quantum yields of **[Bmim]₂SbCl₅**.

Figure S13. IR Spectrum of **[Bmim]₂SbCl₅**.

Figure S14. Optical absorption spectrum of **[Bmim]₂SbCl₅**.

1. Experimental section

Materials and methods

All analytical grade chemicals employed in this study were commercially available and used without further purification. Elemental analyses (EA) for C, H, N were performed on a German Elementary Vario EL III instrument. Fourier transform infrared (FT-IR) spectra were taken on a Nicolet Magna 750 FT-IR spectrometer in the 4000–400 cm⁻¹ region by using KBr pellets. Powder X-ray diffraction (PXRD) patterns was recorded in the angular range of $2\theta = 5-50^\circ$ on a Miniflex II diffractometer using CuK α radiation. Thermogravimetric analyses were carried out with a NETZSCH STA 449F3 unit at a heating rate of 10 °C /min under a nitrogen atmosphere. Emission and excitation

spectra of the compounds were recorded on a PerkinElmer LS55 luminescence spectrometer. The quantum yield measurements were performed on FLS920 produced by EDINGBURGH INSTRUMENTS by means of an integrating sphere. The absolute error on the quantum yield values is about $\pm 1\%$. The compound was excited at a wavelength of 370 nm. The decay time were performed on FLS980 produced by EDINGBURGH INSTRUMENTS.

Synthesis of [Bmim]₂SbCl₅

Heating a mixture of 6 mmol [Bmim]Cl, 3 mmol SbCl₃ and 1 mL ethanol in a vial at 70 °C for 10 minutes resulted in a clear and pale yellow solution. After being cooled to room temperature, light yellow crystals of **1** were slowly precipitated out from the solution. The yield was about 1.25 g, 72% based on SbCl₃. Anal. Calc. for SbCl₅C₁₆H₃₀N₄: C, 33.28%; N, 9.70%; H, 5.24%; Found: C, 32.91 %; N, 9.69%; H, 5.35%.

Single-crystal structure determination.

A suitable single crystal of compound **1** was carefully selected under an optical microscope and glued to a thin glass fiber. The single-crystal diffraction data were collected on a SuperNova CCD diffractometer with graphite-monochromated MoK α radiation ($\lambda = 0.71073$ Å) at 100(2) K. The structure was solved by direct methods and refined by full-matrix least-squares on F^2 by using the programs SHELX-97.¹ All non-hydrogen atoms were refined anisotropically. Hydrogen atoms attached to C atoms were located at geometrically calculated positions and were not refined. The empirical formula were confirmed the element analyses (EA) results. CCDC 1031043, sequentially, contain the supplementary crystallographic data for this paper. Details of crystallographic data and structural refinement parameters are summarized in Table S1.

Table S1. Crystallographic data for [Bmim]₂SbCl₅ (1).

Empirical formula	C ₁₆ H ₃₀ N ₄ Cl ₅ Sb
Formula Mass	577.44
Crystal system	monoclinic
Space group	<i>Cc</i>
<i>a</i> /Å	15.3778(3)
<i>b</i> /Å	27.5062(5)
<i>c</i> /Å	17.4435(3)
α /°	90.00
β /°	102.004(2)
γ /°	90.00
<i>V</i> /Å ³	7217.0(2)
<i>Z</i>	12
<i>T</i> /K	100(2)
Flack parameter	0.325(9)
<i>F</i> (000)	3480

$\rho_{\text{calcd}}/\text{g cm}^{-3}$	1.594
μ/mm^{-1}	1.711
Measured refls.	31310
Independent refls.	14256
No. of parameters	715
R_{int}	0.0267
$R_1 (I > 2\sigma(I))^{\text{a}}$	0.0227
$wR(F^2) (I > 2\sigma(I))^{\text{b}}$	0.0526
GOF	1.000

[a] $R_1 = \sum \|F_o\| - \|F_c\| / \sum \|F_o\|$, [b] $wR_2 = [\sum w(F_o^2 - F_c^2)^2 / \sum w(F_o^2)^2]^{1/2}$.

2. More structure details

Table S2. Selected hydrogen bonding data for [Bmim]₂SbCl₅ (**1**)

D---H...A	D-H (Å)	H...A	D...A	<(DHA) (°)
C(4) --H(4A)...Cl(14) ⁱ	0.98	2.69	3.653(3)	168
C(10) --H(10A)...Cl(8)	0.95	2.78	3.670(4)	156
C(11) --H(11A)...Cl(5)	0.95	2.79	3.658(3)	153
C(16) --H(16A)...Cl(12) ⁱ	0.98	2.67	3.481(3)	140
C(18) --H(18A)...Cl(13) ^v	0.95	2.86	3.597(5)	134
C(20) --H(20B)...Cl(1) ^{iv}	0.98	2.87	3.650(5)	137
C(20) --H(20A)...Cl(1) ⁱⁱ	0.98	2.72	3.625(3)	154
C(22) --H(22A)...Cl(3) ⁱⁱ	0.99	2.84	3.628(4)	137
C(25) --H(25A)...Cl(2)	0.95	2.77	3.671(3)	159
C(28) --H(28A)...Cl(13)	0.98	2.67	3.637(3)	169
C(33) --H(33A)...Cl(14)	0.95	2.86	3.562(5)	131
C(35) --H(35A)...Cl(6)	0.95	2.83	3.616(5)	140
C(37) --H(37A)...Cl(10)	0.99	2.83	3.587(3)	134
C(40) --H(40B)...Cl(13) ⁱⁱ	0.98	2.85	3.655(5)	140
C(40) --H(40A)...Cl(8) ⁱⁱⁱ	0.98	2.62	3.505(3)	151
C(43) --H(43A)...Cl(9)	0.95	2.75	3.628(3)	153
C(48) --H(48A)...Cl(2)	0.98	2.65	3.519(3)	148

Symmetric codes: i: $x, -y, 1/2+z$; ii: $1/2+x, 1/2-y, -1/2+z$; iii: $x, 1-y, -1/2+z$;

iv: $x+1/2, -y+1/2, z+1/2$; v: $x+1/2, y+1/2, z$.

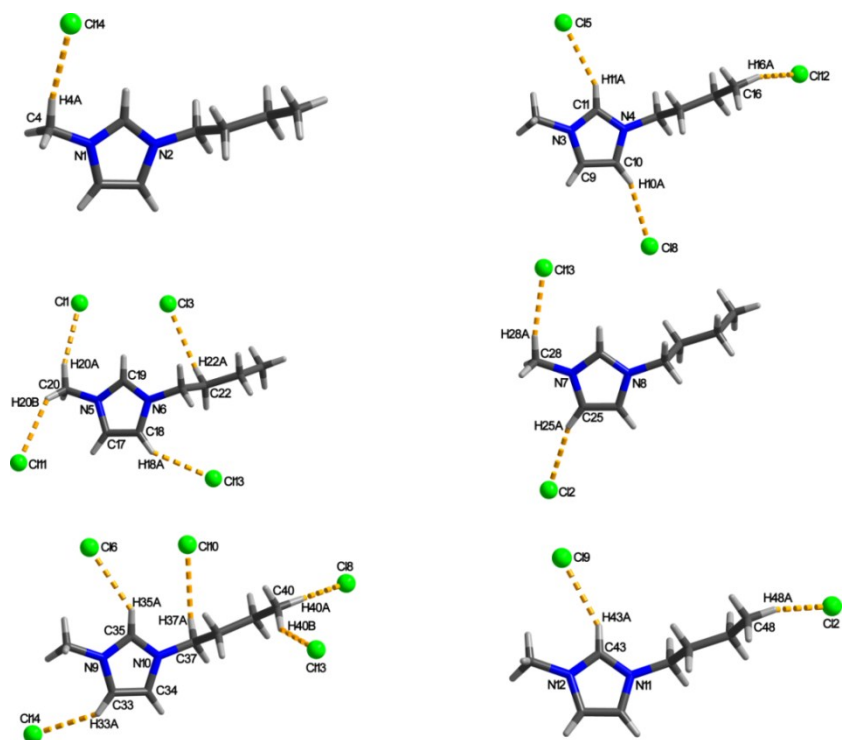


Figure S1. Hydrogen bonds for each imidazolium cation in **1**.

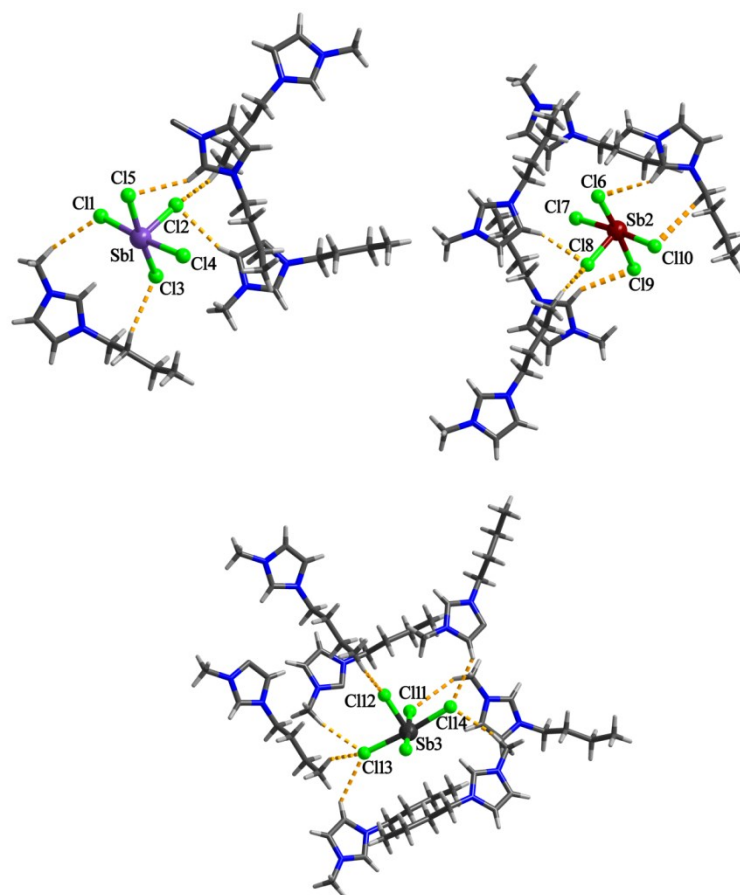
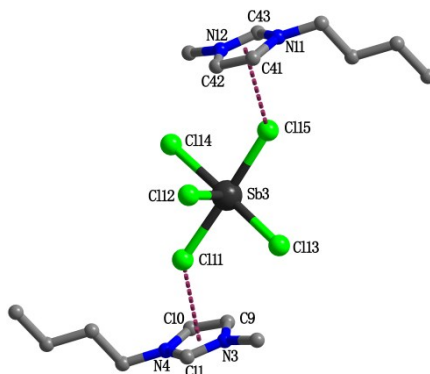


Figure S2. Hydrogen bonds for each $[\text{SbCl}_5]^{2-}$ anion in **1**.

Table S3. Selected Anion- π Interactions data for [Bmim]₂SbCl₅

Y--X(I) Cg(J)	X··Cg(Å)	<Y-X··Cg(°)	Y··Cg(Å)	γ
Sb(3)-Cl(11) → Cg(2)	3.7098(19)	132.21(4)	5.7922(16)	24.25
Sb(3)-Cl(15) → Cg(6)	3.8338(19)	133.27(3)	5.9431(17)	26.93

Cg(2): N(3) → C(9) → C(10) → N(4) → C(11); Cg(6): N(11) → C(41) → C(42) → N(12) → C(43)

**Figure S3.** The anion- π interactions in the molecule. Hydrogen atoms around carbon atoms are omitted for clarity.**Table S4.** Structure diagram of SbX₅²⁻

[SbCl ₅] ²⁻	isolated	
[Sb ₂ X ₁₀] ⁴⁻ (or close to [Sb ₂ X ₁₀] ⁴⁻)	dimerization	
[Sb ₄ X ₂₀] ⁸⁻	tetrameric	
[Sb ₂ Cl ₅] _n ⁻²ⁿ	anion chain	

Table S5. Selected Bond lengths for [Bmim]₂SbCl₅ (**1**).

C(1)-C(2)	1.353(5)
C(5)-C(6)	1.513(5)
C(6)-C(7)	1.511(4)
C(7)-C(8)	1.536(5)
C(9)-C(10)	1.343(5)
C(13)-C(14)	1.507(4)
C(14)-C(27)	1.512(4)
C(16)-C(27)	1.529(5)
C(17)-C(18)	1.356(5)
C(21)-C(22)	1.524(5)
C(22)-C(23)	1.524(4)
C(23)-C(24)	1.518(4)
C(25)-C(26)	1.343(5)
C(29)-C(30)	1.515(5)
C(30)-C(31)	1.522(4)
C(31)-C(32)	1.513(4)
C(33)-C(34)	1.341(6)
C(37)-C(38)	1.507(4)
C(38)-C(39)	1.519(4)
C(39)-C(40)	1.518(4)
C(41)-C(42)	1.355(5)
C(45)-C(46)	1.517(4)
C(46)-C(47)	1.522(4)
C(47)-C(48)	1.523(5)

3. Theoretical calculations

Calculation method

All the calculations were implemented in Gaussian 09 program.² The density functional theory (DFT) method at the hybrid Becke three-parameter Lee-Yang-Parr (B3LYP)³ functional level was used for the geometrical optimization of [Bmim]⁺ and [SbCl₅]²⁻ in the ground states, respectively. While the optimization processes of lowest singlet excited states of them were implemented by time-dependent DFT (TD-DFT)⁴ at the same functional. Then, 20 singlet excited states were calculated to determine the emission energies of [Bmim]⁺ and [SbCl₅]²⁻ by TD-DFT method based on the optimized structures in the lowest singlet excited states, respectively. In these calculations, the Lan12dz⁵ effective core potential was used to describe the inner electrons of Sb atom, while its associated double- ζ basis set of

Hay and Wadt was employed for the remaining outer electrons. And all-electron basis set of 6-31+G** was used for the non-metal atoms of Cl, N, C, and H. Visualization of the optimized structures and the frontier molecular orbitals were performed by GaussView.

Table S6 Plots of the frontier molecular orbitals involved in the emission transitions of **[Bmim]⁺** and **[SbCl₅]²⁻** calculated by TD-DFT method at the B3LYP level (isovalue = 0.03).

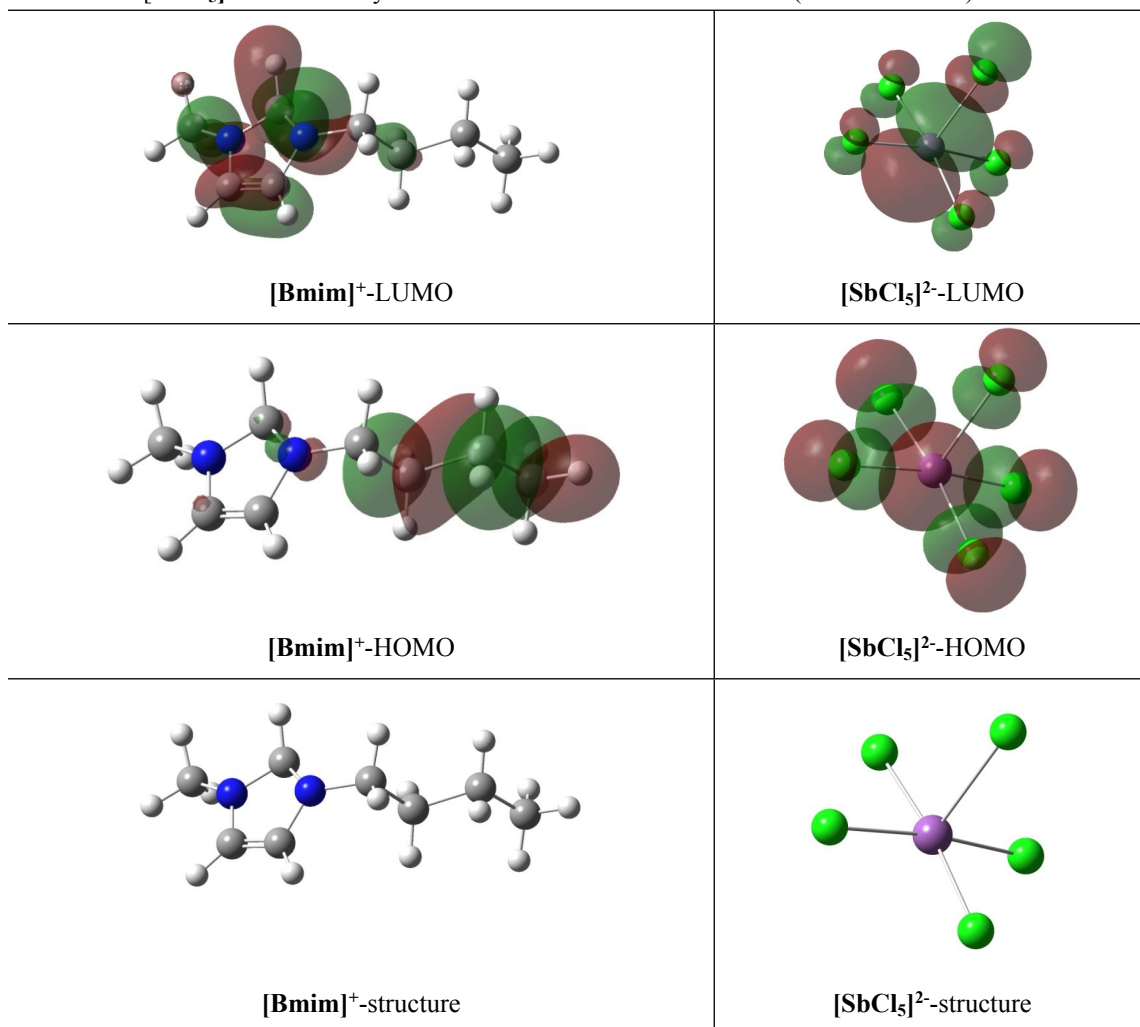


Table S7 The optimized geometrical coordinates (unit: angstroms) of **[SbCl₅]²⁻** in the ground state by DFT method at the B3LYP level.

center number	atomic type	coordinates		
		x	y	z
1	Sb	0	0	0.213661
2	Cl	0	0	-2.29151
3	Cl	0	2.740515	0.412632
4	Cl	-2.74052	0	0.412632
5	Cl	2.740515	0	0.412632
6	Cl	0	-2.74052	0.412632

Table S8 The optimized geometrical coordinates (unit: angstroms) of $[\text{SbCl}_5]^{2-}$ in the lowest singlet excited state by DFT method at the B3LYP level.

center number	atomic type	coordinates		
		<i>x</i>	<i>y</i>	<i>z</i>
1	Sb	0	0	0.290272
2	Cl	0	0	-2.84213
3	Cl	0	2.686491	0.492827
4	Cl	-2.68649	0	0.492827
5	Cl	2.686491	0	0.492827
6	Cl	0	-2.68649	0.492827

Table S9 The optimized geometrical coordinates (unit: angstroms) of $[\text{Bmim}]^+$ in the ground state by DFT method at the B3LYP level.

center number	atomic type	coordinates		
		<i>x</i>	<i>y</i>	<i>z</i>
1	N	2.548474	-0.19687	-0.15764
2	N	0.490489	0.157483	0.472756
3	C	2.310982	1.159392	-0.28655
4	H	3.067978	1.8436	-0.63699
5	C	1.022669	1.379992	0.106785
6	H	0.451898	2.293728	0.159716
7	C	1.432037	-0.77859	0.302243
8	H	1.313284	-1.83177	0.506675
9	C	3.813921	-0.88048	-0.46575
10	H	3.699574	-1.94511	-0.26337
11	H	4.608691	-0.47477	0.162567
12	H	4.057972	-0.7352	-1.51946
13	C	-0.89835	-0.08378	0.934682
14	H	-1.10308	0.649328	1.71997
15	H	-0.90774	-1.07414	1.397069
16	C	-1.92333	0.008872	-0.20013
17	H	-1.66607	-0.7184	-0.98083
18	H	-1.87129	1.003153	-0.66169
19	C	-3.35083	-0.25	0.307038
20	H	-3.3981	-1.24539	0.768082
21	H	-3.59171	0.470932	1.099344
22	C	-4.39575	-0.15188	-0.81003
23	H	-5.39911	-0.34311	-0.41947
24	H	-4.20266	-0.88311	-1.60259
25	H	-4.40047	0.844784	-1.26463

Table S10 The optimized geometrical coordinates (unit: angstroms) of **[Bmim]⁺** in the lowest singlet excited state by DFT method at the B3LYP level.

center number	atomic type	coordinates		
		x	y	z
1	N	-2.43599	0.368232	-0.00753
2	N	-0.53881	-0.69117	0.51347
3	C	-2.3625	-0.78603	-0.76709
4	H	-3.16002	-1.08085	-1.4315
5	C	-1.2062	-1.42847	-0.47641
6	H	-0.84274	-2.37979	-0.83206
7	C	-1.23485	0.550991	0.706614
8	H	-1.33382	0.899187	1.74128
9	C	-3.43702	1.409287	-0.13992
10	H	-3.68548	1.809655	0.847164
11	H	-4.34227	0.986051	-0.57764
12	H	-3.07834	2.230355	-0.7721
13	C	0.868761	-0.81953	0.812748
14	H	1.125207	-1.88396	0.816477
15	H	1.042687	-0.45218	1.829772
16	C	1.758725	-0.06831	-0.18034
17	H	1.539717	1.021852	-0.21206
18	H	1.691815	-0.44363	-1.20243
19	C	3.292689	0.159209	0.260984
20	H	3.380243	0.434576	1.309617
21	H	3.368308	-0.97814	0.147294
22	C	4.239967	0.824555	-0.65481
23	H	5.276099	0.552769	-0.37149
24	H	4.235618	1.915628	-0.49868
25	H	4.089106	0.578861	-1.70599

Table S11. Partial molecular orbital compositions (%) in the lowest singlet excited state for **[Bmim]⁺** by TD-DFT method at the B3LYP level.

Orbital	MO contribution (%)	
	NN-Me	Butyl
LUMO	86.89	13.11
HOMO	4.81	95.19

Table S12. Partial molecular orbital compositions (%) in the lowest singlet excited state for **[SbCl₅]²⁻** by TD-DFT method at the B3LYP level.

Orbital	MO contribution (%)	
	Sb	Cl

LUMO	64.10	35.90
HOMO	31.35	68.65

Table S13. The emission transitions for $[\text{Bmim}]^+$ and $[\text{SbCl}_5]^{2-}$, respectively, by TD-DFT method at the B3LYP level.

States	E , nm	O.S.	Transition	Contrib.	Assignment	Exp. (nm)
$[\text{Bmim}]^+-S_1$	390	0.0003	HOMO \rightarrow LUMO	100%	ILCT	460
$[\text{SbCl}_5]^{2-}-S_1$	545	0.0154	HOMO \rightarrow LUMO	95%	LMCT	580

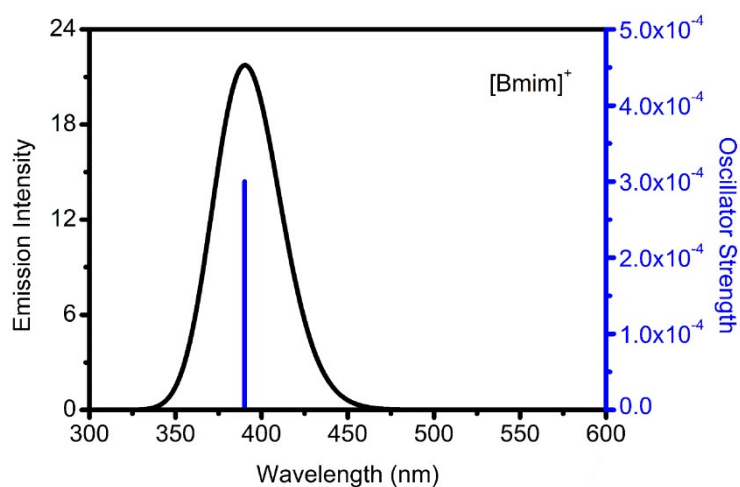


Figure S4 The calculated (blue vertical bars) and simulated (black line, implemented by GaussSum) emission spectra of $[\text{Bmim}]^+$ at ambient temperature calculated by TD-DFT method at the B3LYP level.

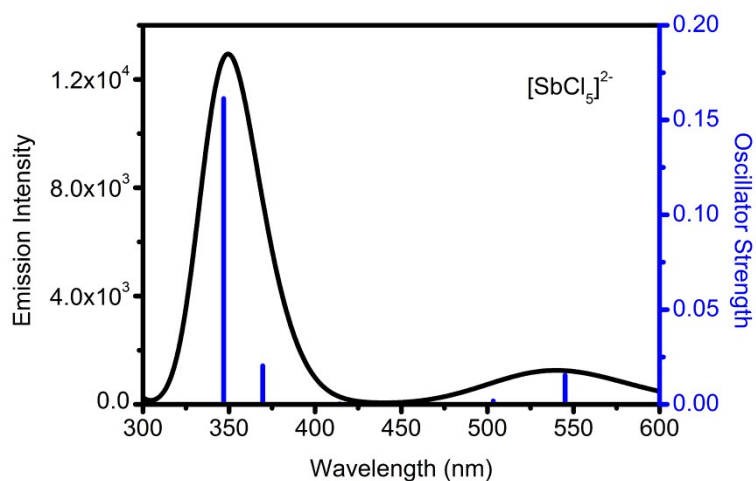


Figure S5 The calculated (blue vertical bars) and simulated (black line, implemented by GaussSum) emission spectra of $[\text{SbCl}_5]^{2-}$ at ambient temperature calculated by TD-DFT method at the B3LYP level.

4. Physical measurements

4a) PXRD

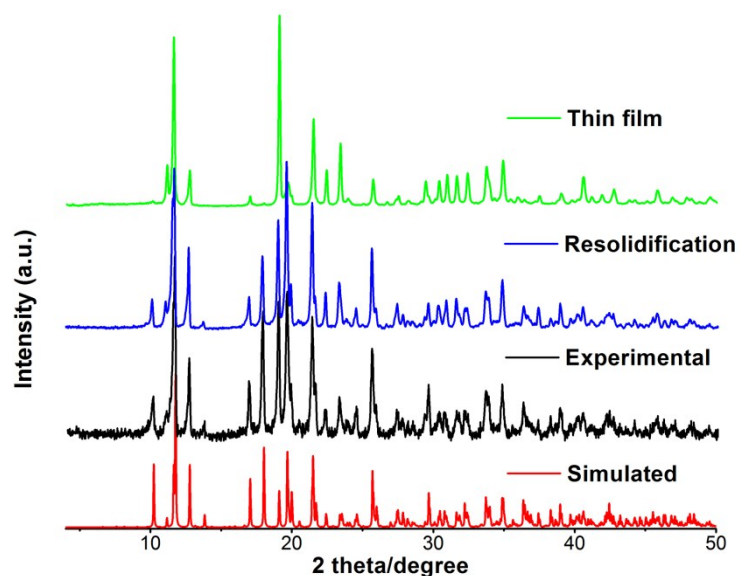


Figure S6 PXRD patterns of [Bmim]₂SbCl₅. The powder pattern of [Bmim]₂SbCl₅ matches quite well with the simulated from single-crystal X-ray data, indicating bulk purity of the compound, and the structure of **1** remained intact after solidification. X-ray diffraction pattern of the film indicates the high degree of crystallinity, and preferred orientation of some higher order reflections.

4b) Photoluminescence lifetime curve

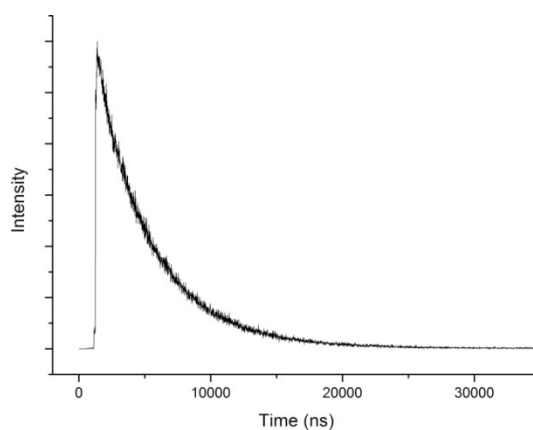


Figure S7 Fluorescence lifetime curve of [Bmim]₂SbCl₅.

4c) TGA

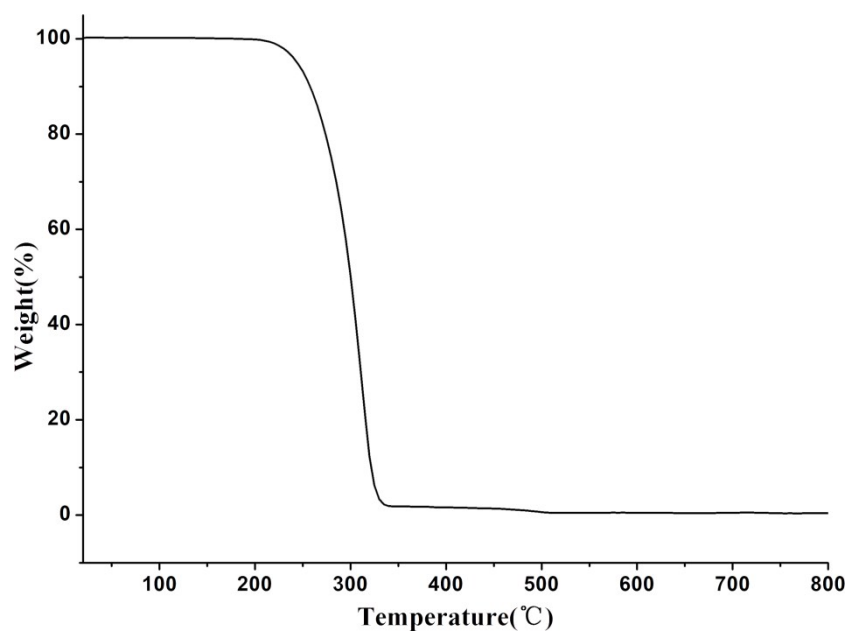


Figure S8 TGA curve of [Bmim]₂SbCl₅. TGA studies of [Bmim]₂SbCl₅ was performed in a N₂ atmosphere from 25 to 800 °C. The TGA curve of the title compound is quite similar with some other ionic liquids. A weight loss of approximate 99% occurred in the temperature range of 230–330 °C (calculated 96.5%), and then the curve showed a long stable plateau up to 330 °C.

4d) DSC

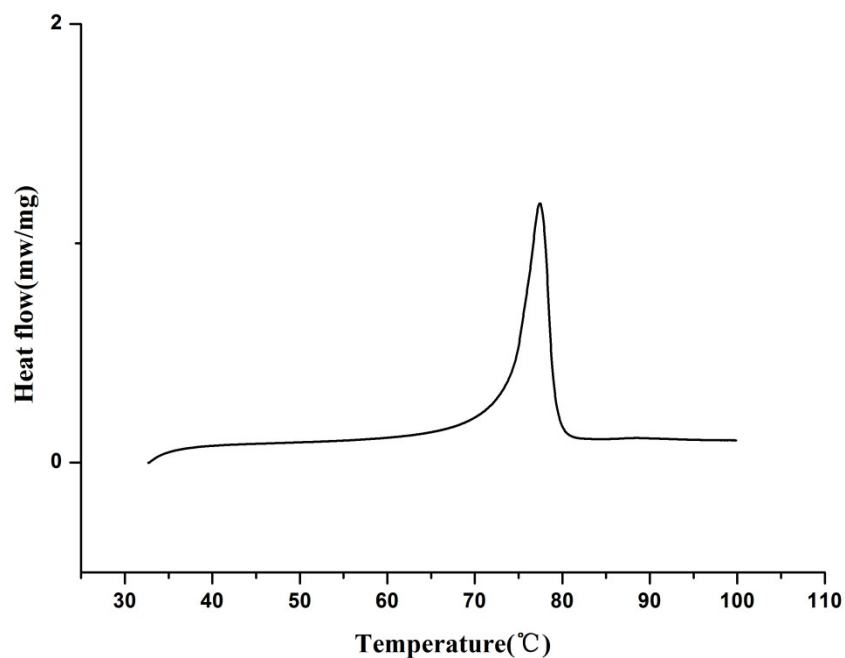


Figure S9 DSC curve of [Bmim]₂SbCl₅.

4e) Temperature-dependent PXRD

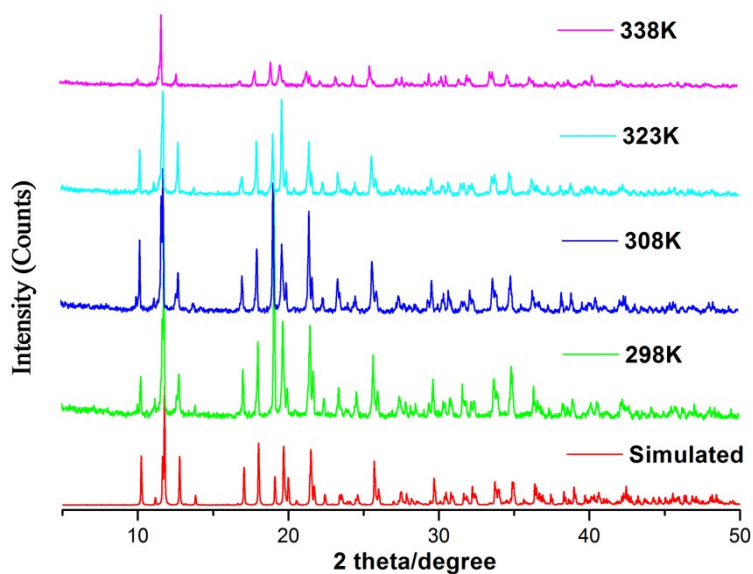


Figure S10 Temperature-dependent PXRD of [Bmim]₂SbCl₅.

4f) Temperature-dependent PL spectra

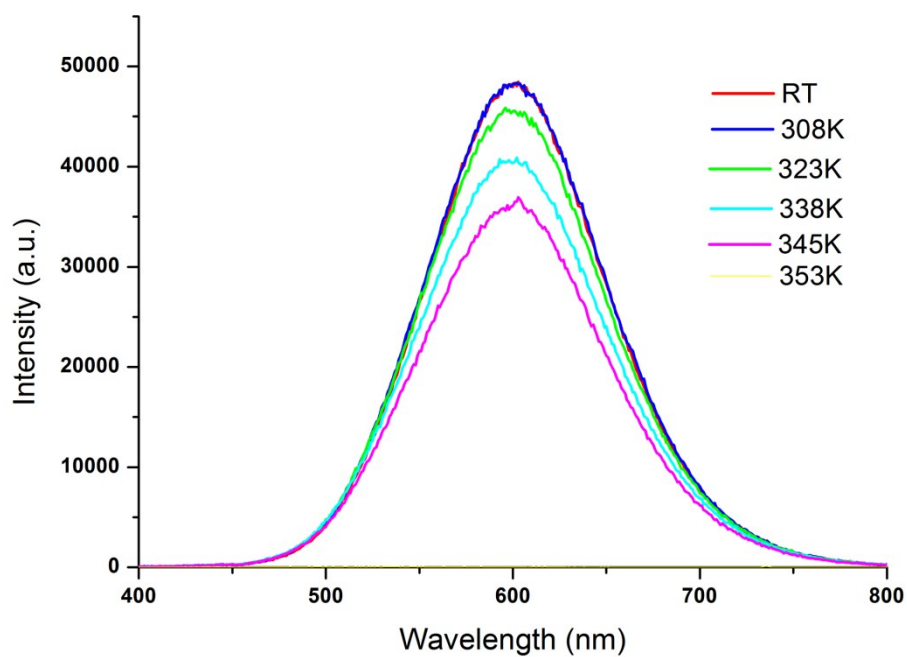


Figure S11 Temperature-dependent PL spectra of [Bmim]₂SbCl₅.

4g) Temperature-dependent QYs

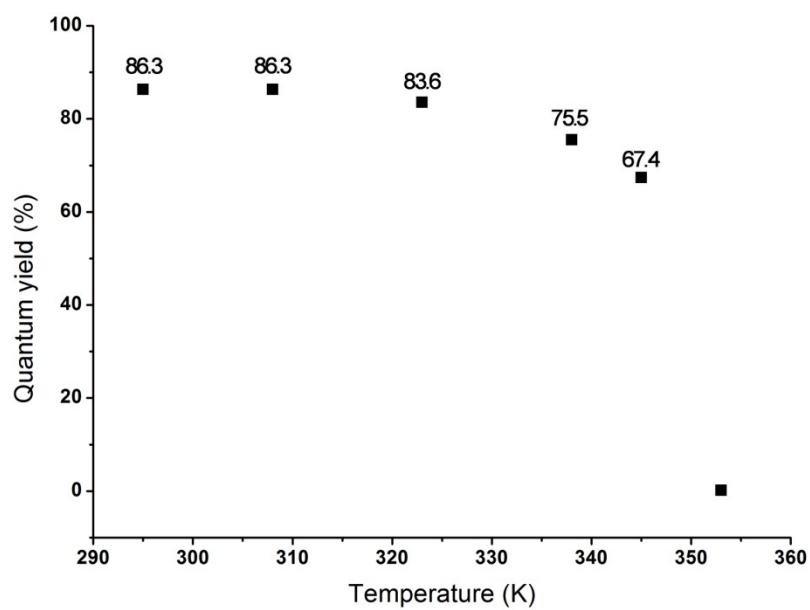


Figure S12 Temperature-dependent QYs of [Bmim]₂SbCl₅.

4h) IR spectrum

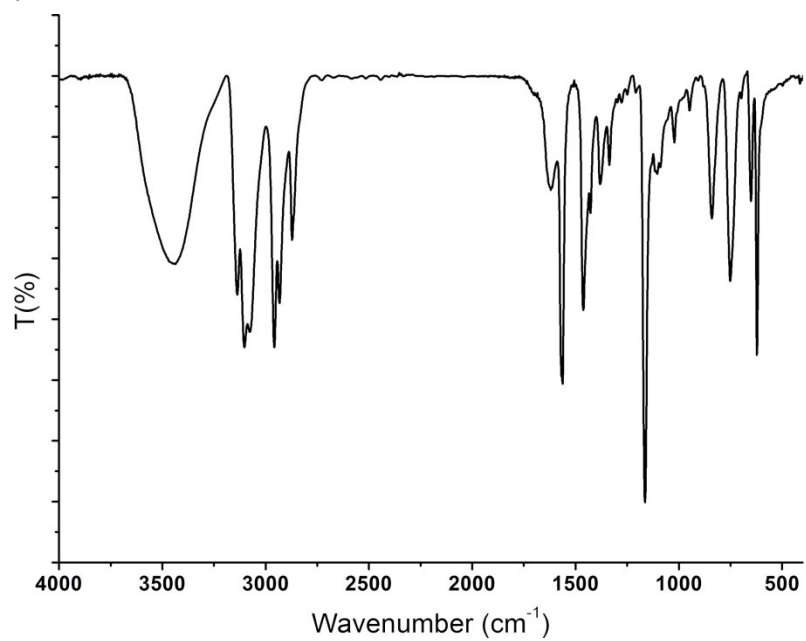


Figure S13 IR Spectrum of [Bmim]₂SbCl₅.

4i) Optical absorption spectrum

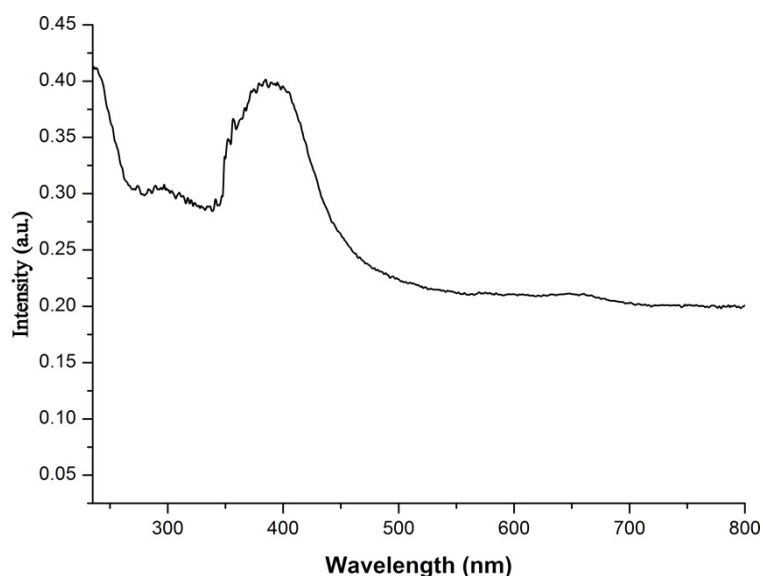


Figure S14 Optical absorption spectra of [Bmim]₂SbCl₅.

References

1. G. M. Sheldrick, *SHELXS97 and SHELXL97*, University of Göttingen, Germany, 1997.
2. M. J. Frisch, G. W. Trucks, H. B. Schlegel, G. E. Scuseria, M. A. Robb, J. R. Cheeseman, G. Scalmani, V. Barone, B. Mennucci, G. A. Petersson, H. Nakatsuji, M. Caricato, X. Li, H. P. Hratchian, A. F. Izmaylov, J. Bloino, G. Zheng, J. L. Sonnenberg, M. Hada, M. Ehara, K. Toyota, R. Fukuda, J. Hasegawa, M. Ishida, T. Nakajima, Y. Honda, O. Kitao, H. Nakai, T. Vreven, J. A. Montgomery, Jr., J. E. Peralta, F. Ogliaro, M. Bearpark, J. J. Heyd, E. Brothers, K. N. Kudin, V. N. Staroverov, T. Keith, R. Kobayashi, J. Normand, K. Raghavachari, A. Rendell, J. C. Burant, S. S. Iyengar, J. Tomasi, M. Cossi, N. Rega, J. M. Millam, M. Klene, J. E. Knox, J. B. Cross, V. Bakken, C. Adamo, J. Jaramillo, R. Gomperts, R. E. Stratmann, O. Yazyev, A. J. Austin, R. Cammi, C. Pomelli, J. W. Ochterski, R. L. Martin, K. Morokuma, V. G. Zakrzewski, G. A. Voth, P. Salvador, J. J. Dannenberg, S. Dapprich, A. D. Daniels, O. Farkas, J. B. Foresman, J. V. Ortiz, J. Cioslowski, and D. J. Fox, Gaussian, Inc., Wallingford CT, 2013.
3. (a) C. T. Lee, W. T. Yang, R. G. Parr, *Phys. Rev. B* 1988, **37**, 785-789; (b) A. D. Becke, *J. Chem. Phys.* 1993, **98**, 5648-5652.
4. R. Bauernschmitt, R. Ahlrichs, *Chem. Phys. Lett.* 1996, **256**, 454-464. (b) M. E. Casida, C. Jamorski, K. C. Casida, D. R. Salahub, *J. Chem. Phys.* 1998, **108**, 4439-4449. (c) R. E. Stratmann, G. E. Scuseria, M. J. Frisch, *J. Chem. Phys.* 1998, **109**, 8218-8224.
5. (a) P. J. Hay, W. R. Wadt, *J. Chem. Phys.* 1985, **82**, 270-283. (b) W. R. Wadt, P. J. Hay, *J. Chem. Phys.* 1985, **82**, 284-298. (c) P. J. Hay, W. R. Wadt, *J. Chem. Phys.* 1985, **82**, 299-310.